ORIGINAL ARTICLE

Evolution and effect of the stress concentration and rock failure in the deep multi-seam coal mining

Mingwei Zhang · Hideki Shimada · Takashi Sasaoka · Kikuo Matsui · Linming Dou

Abstract Supports crushing accident occasionally occurs in the protected seam exploitation of deep multi-seam coal mining structure and results in adverse effect to the production. To prevent its recurrence in a newly developed working field, a 3D numerical extraction model was built based on the geologic and mining conditions of Jining coal mine to evolve the changes, state and characteristics of the reconstructed vertical and lateral stress in rock interlayer after protective seam exploitation. Stress release and increase zones of this mining structure were separated. Mining-induced localized stress concentration and the interlayer rock failure behavior were explored. The action of concentrated stress on the hydraulic supports in protected seam was discussed upon the major stress redistribution. Using the infinitesimal strain method, a mechanical model was created to further explore, from the vertical and lateral directions, the cause and mechanism of localized stress concentration and rock failure behavior in rock interlayer. The field investigation was finally performed to verify the numerical and mechanical results, and the essential control measures were proposed to prevent this accident. Key findings of this study bring some new insights into the deep multi-seam coal extraction and help to promote a more reliable underground mining.

Introduction

The multi-seam mining method has been widely applied in underground coal mines for many years. It changes the initial distribution of in situ stress in the deep country rock, improves the plastic deformation of coal and rock mass, weakens the stress concentration degree in the mining region and makes the other coal seams easier to be extracted (Tati 2011; Khare et al. 2006; Nasedkina et al. 2009; Wang and Zhao 2010; Yang et al. 2011a, b, c). The first mined coal seam is usually named the protective seam. Because it provides favorable mechanical conditions, the second mined coal seam is defined as the protected seam. In early application, this method was used to control the coal outburst in the gas-enriched shallow seams (Liu et al. 2011; Yang et al. 2011a, b, c). The protective seam exploitation was one of the most effective and economical methods to eliminate the coal and gas outburst in protected seam (Xiong et al. 2008). Reasonable gas extraction measures in the protective seam played an important role in the regional control of these hazards (Yang et al. 2011a, b, c). With the increase of mining depth, more hazardous geologic phenomena such as the high underground temperature and pressure gradually appear and seriously hamper the safe mining (Lobanova 2008). Accordingly, the multi-seam mining method is deeply developed for the geological hazard prevention in recent years. It indicates that one of the multiple coal seams should be extracted first if it is nonhazardous or relatively low hazardous (Dou et al. 2006). The exploitation of protective seam is recognized as

M. Zhang (✉) · H. Shimada · T. Sasaoka · K. Matsui
Department of Earth Resources Engineering,
Faculty of Engineering, Kyushu University, 744 Motooka,
Nishi-ku, Fukuoka 819-0395, Japan
e-mail: mingwei11r@mine.kyushu-u.ac.jp

L. Dou
School of Mines, China University of Mining and Technology,
Xuzhou 221008, China

a more necessary and effective precautionary approach for the deep hazard control. It is normally given a higher priority to improve the stress conditions in the working field (China Ministry of Coal Industry 1987).

In multi-seam mining structure, the region that is over and under the goaf of protective seam is usually considered the stress release zone. Protected seam exploitation in the stress release zone should generally be more secure than the mining activities in other regions. However, in the deep production conditions, the protected seam exploitation is sometimes not as easy and smooth as expected. Some abnormal mining accidents occasionally occurred. For instance, the bolts and the cables in rock roof frequently snapped, and the roadway near the working face badly deformed. In particular, some hydraulic supports located in the middle working face were tightly crushed. These abnormal phenomena delayed the mining schedule, destroyed the hydraulic supports, and threatened the miners' life security in the worst cases (Nasedkina et al. 2008; Qin et al. 2006; Yin et al. 2012), which cause serious direct and indirect losses to the deep mines and make the protected seam extraction inconsistent with the general opinion. It is without doubt a matter of great concern.

Recent researches on multi-seam coal mining mainly focus on the dynamic stress evolution surrounding the working faces, the determination of pressure releasing angle and safe mining region, and the optimized layout of roadways in the protected seam (Guo et al. 2012; Zhang et al. 2011; Yuan et al. 2010). The possible stress concentration behavior in the rock interlayer of the multi-seam mining structure and its direct effect on the mining feasibility in protected seam are rarely discussed. Because the multi-seam mining method will be widely applied in the deeper underground coal mines, the relevant studies on this point become necessary for the better accident prevention. In allusion to the problems mentioned, the authors of this study deduced that these abnormal mining accidents are closely related to the stress concentration behavior reconstructed in the rock interlayer. It is known that in situ stress decreases in the stress release zone. However, the reconstruction of major stress does not imply that both its vertical and lateral components decrease simultaneously. It seems possible that in a specific region, the vertical stress sharply decreases, whereas the lateral stress slightly increases. Thus, once the lateral stress increases to a high level, it would result in the localized stress concentration and cause these adverse effects to the coal extraction activity in the protected seam.

In this research work, to confirm the inference, a numerical coal extraction model was built by the Fast Lagrangian Analysis of Continua in 3 Dimensions (FLAC3D) based on the geological and mining conditions in a multi-seam mining field to evolve the changes and characteristics of reconstructed stress in the rock interlayer after the protective seam exploitation. Following that, a mechanical model was created using the infinitesimal strain method to further explore the cause and mechanism of localized stress concentration and rock failure behavior in the rock interlayer of the multi-seam mining structure and to elaborate the mechanical factors that result in the mining accidents. Field investigation in corresponding mining field was then carried out to verify the numerical and mechanical analysis, and some essential control measures were finally proposed for the abnormal accident prevention. Here, the authors expound the research organization and propose the valuable theoretical and practical experience about the localized stress concentration behavior in rock interlayer and its impact on deep multi-seam coal mining.

Mining conditions and model development

Underground mining conditions

Jining coal mine located in the East China district is a deep underground mine. With the increase in mining depth, this mine gradually faces some hazards induced from the high ground pressure. Hence, the multi-seam mining method is applied to prevent and control those hazards effectively in the multiple coal seams zone. However, despite its advantages, the coal extraction activities in protected seam were always suspended by the supports crushing accidents, which led to an extremely adverse effect on the principle of safe mining.

The TZ working field is one of the multi-seam mining fields. It is a newly developed field, where the upper and the lower coal seams are named the TZU and the TZL seams, respectively. Overburden depth of the TZU seam is approximately −620 m. Thickness of two coal seams is 2.85 and 5.0 m, and their interlayer spacing is 42.7 m in average. The interlayer rock mass is a type of gray compact sandstone with a few fractures developed. Mining layout of the TZ working field and its geologic column are shown in Fig. 1. In general, coal seam occurrence in this field is steady. The terrain is relatively high in the southwest zone. The significant geological tectosome consists mainly of a huge gentle monocline plunging towards the northeast and three major normal faults dissecting the mining field, which play a preparative role in the in situ stress distribution in country rock of the mining area. In situ stress conditions of the TZ working field were separately measured in the upper and lower coal seams, and the measured results are listed in Table 1. The longwall mining is used to exploit the full seam. Face TZU04, 2,450 m in length and 180 m in width, is located in the middle region and is firstly extracted.
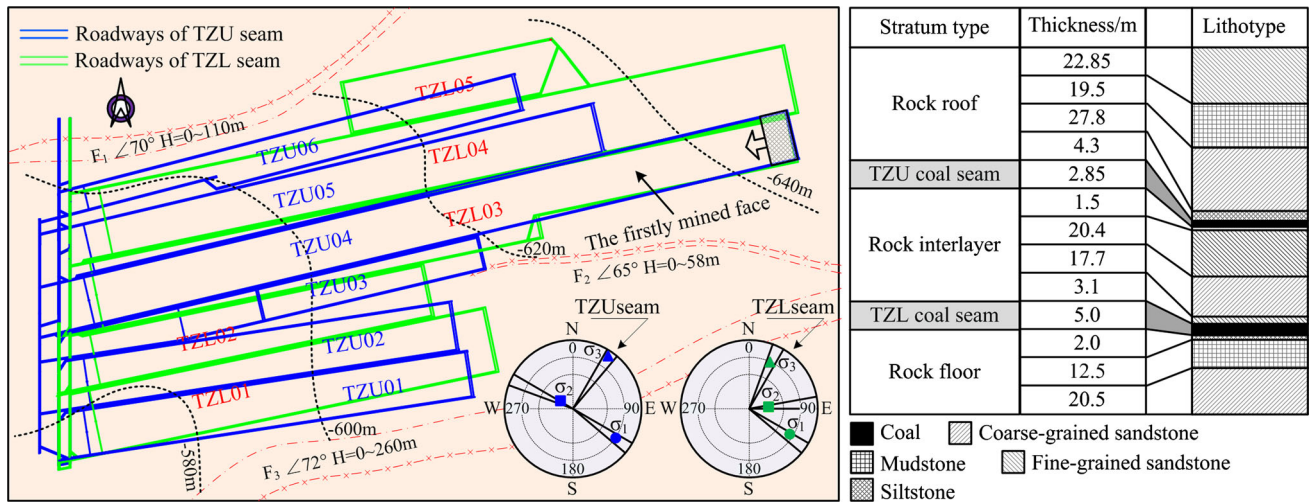
Fig. 1 Layout of the TZ working field and the relevant geological column

Table 1 In-situ stress value measured in the field

Stress (MPa)/Azimuth angle (°)	$\sigma 1$	$\sigma 2$	$\sigma 3$
TZU coal seam	16.5/123	10.45/290	8.27/33
TZL coal seam	17.9/120	8.81/86	5.68/24

Developing a coal extraction model

To prevent those abnormal mining accidents from reoccurring in this new working field, it is necessary to thoroughly understand the rules and characteristics of the stress reconstruction in the rock interlayer after the protective seam exploitation and explore its effect on the coal extraction activity in protected seam. Hence, the numerical simulation was introduced into this study. The numerical coal extraction model of Face TZU04 was developed using the finite difference program FLAC3D. This software is an important computer-aided analysis tool in the field of rock mechanics. By establishing the constitutive equations of engineering materials, the model calculation effectively traces the gradual failure process of elastic and plastic structures such as the coal body and the rock mass. Its geometric equations are appropriate for solving the non-linear problems with a large deformation (Itasca Consulting Group, Inc, 2005).

Length, width and height of the coal extraction model were 500, 280 and 160 m, respectively, and 775,200 finite elements were applied. Model parameters were extracted from the mining and geologic conditions of the TZ working field. The mining parameters were explored as previously mentioned; the geologic parameters were obtained based on the physical and mechanical property tests of coal and rock specimen in laboratory as shown in Fig. 2. The applied coal and rock properties are listed in Table 2.

Based on the measured in situ stress value, the ground pressure gradient and the lateral-to-vertical stress ratio were identified to be approximately 26.5 kPa/m and 1.7, respectively. Considering the restriction of model dimensions, a 13.9 MPa compressive stress was loaded upon its top surface to evolve the initial pressure environment. The developed numerical extraction model is shown in Fig. 3.

Compared to the TZL seam, the TZU seam is shallowly buried and relatively low hazardous. Thus, it is perceived as the protective seam to eliminate the effect of high ground pressure. Mining activity in Face TZU04 is the initial disturbance and destruction to the rock interlayer, which minimizes the external influence induced from other mining or geological factors.

Results and discussion

Stress release zone of the deep multi-seam mining structure

Before the protective seam exploitation, stress in the deep surrounding rock mass remained in an equilibrium state. This state was broken by the coal extraction activity in Face TZU04. Stress reconstructed in a wide region and finally reached a new balanced state. Mining region affected by the stress reconstruction is artificially divided into three different zones: the stress release zone, the stress increase zone and the stress stable zone (Yang et al. 2011a, b, c). This division is established on the relationship of reconstructed stress and its initial value. The region is defined as the stress release zone if the reconstructed stress is lower than its initial value. Conversely, it is treated as the stress increase zone. Reconstructed stress used for this division is determined by the vertical component of major

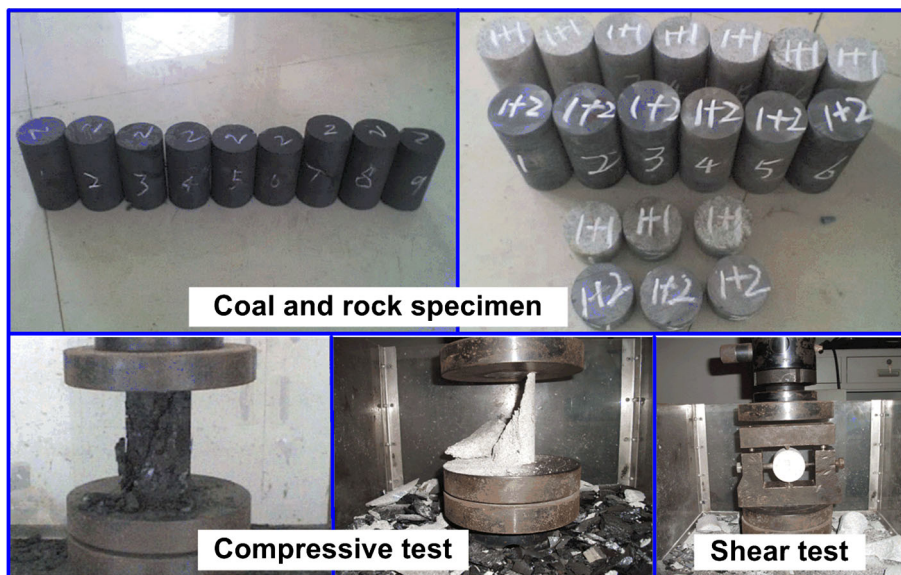**Fig. 2** Mechanical property tests of coal and rock specimen

Coal and rock specimen

Compressive test

Shear test

Table 2 Coal and rock properties applied in the numerical extraction model

	Coal	Mudstone	Coarse-grained sandstone	Fine-grained sandstone	Siltstone
Density (kg m^{-3})	1,380	2,655	2,709	2,753	2,730
Moisture content (%)	3.52	2.49	2.62	1.76	2.68
Compressive strength (MPa)	15.83	47.55	64.69	117.37	88.77
Shear strength (MPa)	14.19	19.91	18.53	57.96	38.44
Tensile strength (MPa)	1.06	3.89	5.58	6.29	4.3
Elastic modulus (GPa)	12.21	28.19	37.6	81.45	46.67
Cohesion (MPa)	6.2	13	16	24	22
Poisson ratio	0.27	0.13	0.15	0.19	0.14
Angle of internal friction (°)	26.9	22	18.4	31	24

Fig. 3 Numerical extraction model of the deep multi-seam coal mining structure

Unit: m
Model size: (L)500×(W)280×(H)160
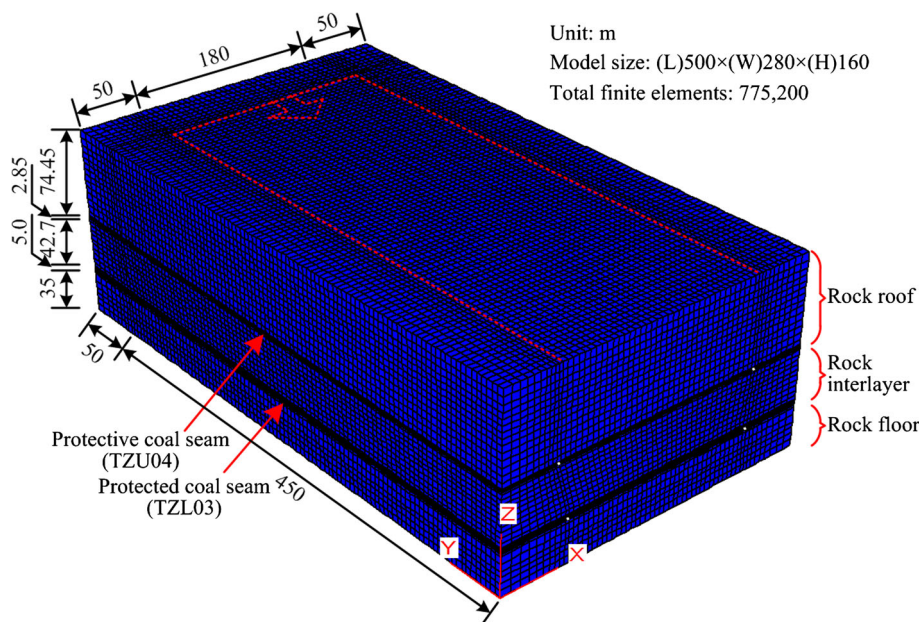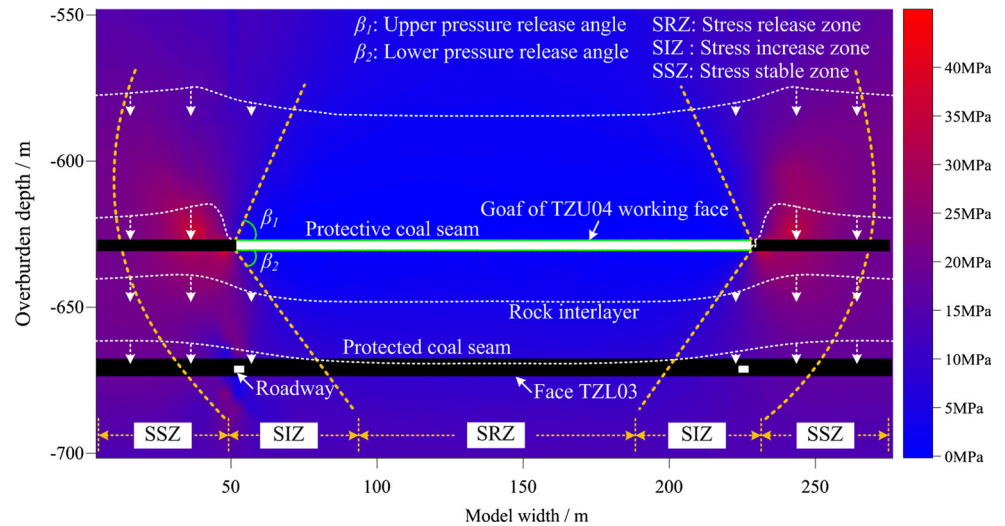Total finite elements: 775,200

Fig. 4 Three disparate stress zones in the multi-seam mining structure after protective seam exploitation

stress. These disparate stress zones around the TZU04 goaf are shown in Fig. 4. For this multi-seam mining structure, the stress redistribution is almost symmetrical in the direction parallel to the working face. It shows that the protective seam exploitation dramatically lowers the stress level in the region under the TZU04 goaf. Thus, this region is the stress release zone of this mining structure, which provides the positive mechanical conditions for the further coal extraction in Face TZL03.

Changes of vertical stress in the rock interlayer

Major stress distribution in deep rock mass is ubiquitous and complicated (Sun et al. 2013; Wu and Pan 2013). It is always decomposed into the vertical component (Szz) and the lateral component (Sxx) based on the parallelogram rule. They are two significant parameters expected to be obtained in application (Lempp et al. 2012; Lourenco et al. 2011; Hashash et al. 2002). Concentration degree of the reconstructed stress is defined by the expression $f_c = S_r/S_i$, where f_c is the effective stress concentration factor, and S_i and S_r are the initial stress and the reconstructed stress, respectively. Vertical stress level in the rock interlayer mirrored by the stress concentration factor is shown in Fig. 5. It shows that vertical stress increases apparently ($f_c > 1$) and concentrates on the upper interlayer rock mass under the virgin protective coal seam, which is mainly induced by the stress transfer in the rock roof. In the stress release zone, the vertical stress decreases significantly ($f_c < 1$) but increases slightly with the overburden depth as the comparison results shown in cross sections A–A, B–B and C–C. It is noted that a residual stress acts upon the top surface of rock interlayer as the caving rock roof in the TZU04 goaf. Residual stress varies with the location and amount of the caving rock mass. Because of the obvious decrement, vertical stress becomes a primary impact factor for the underground pressure release and attracts more attention in application (Jia et al. 2013; Gurbuz 2011).

Changes of lateral stress in the stress release zone of rock interlayer

Lateral stress level in the rock interlayer mirrored by the relevant stress concentration factor is shown in Fig. 6. It shows that lateral stress mainly concentrates at two regions. One is located at the interface between the upper interlayer rock mass and the virgin protective coal seam, which is similar to the concentration state of vertical stress. Another is located at the bottom of rock interlayer, under the middle goaf. Along the borderline of TZU04 goaf, lateral stress sharply increases and then gradually decreases to a lower level (cross sections D–D and F–F). This changes result from the former stress concentration behavior. However, lateral stress changes following a dissimilar rule along the goaf centerline. It increases gradually to a higher level and then declines sharply at the immediate roof of protected seam (cross section E–E). The peak stress value here is lower than that on the borderline. Lateral stress changes in the stress release zone can be separated into three gradients. The first gradient (G1) is located at the upper and middle parts of the rock interlayer, where the lateral stress decreases and is less than its original value ($f_c < 1$). The second gradient (G2) is located at its lower-middle part, where the lateral stress is a little higher than its original value ($1 \le f_c < 1.5$). The third gradient (G3) is located at its lower part. Lateral stress in this region is obviously greater than its original value, i.e., $f_c \ge 1.5$. It indicates that the changes of lateral stress are affected by the released vertical stress to some extent. However, it greatly increases with the overburden depth and highly concentrates in the lower part of rock interlayer.
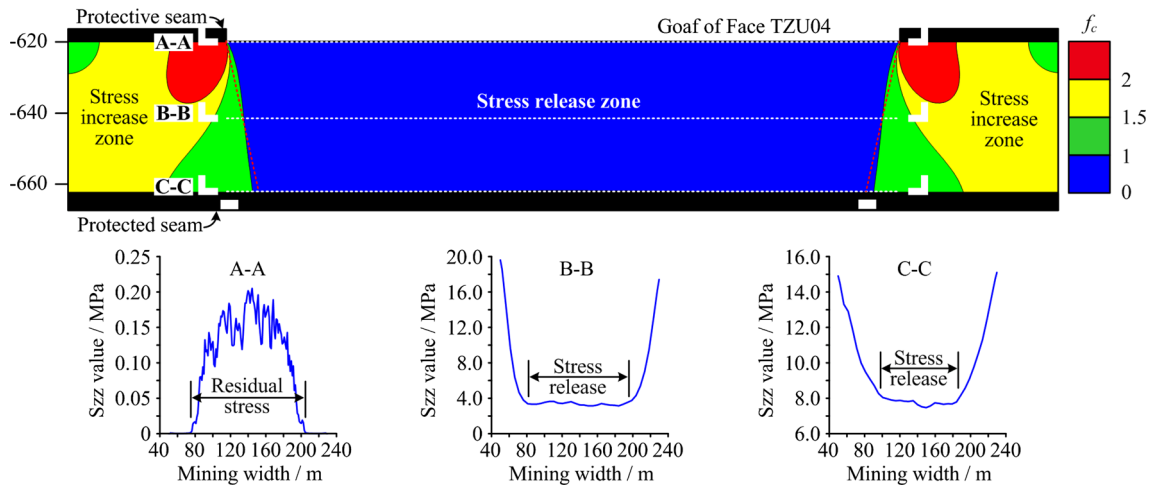
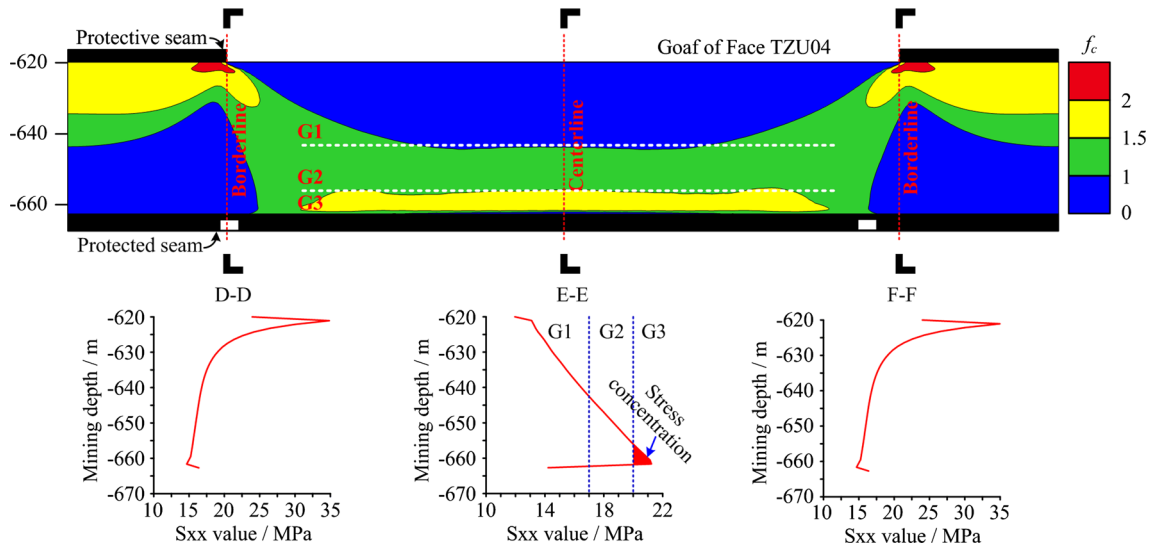Fig. 5 Concentration degree of the vertical stress in rock interlayer

Fig. 6 Concentration degree of the lateral stress in rock interlayer

Mining-induced localized stress concentration in rock interlayer

Comparative redistribution of the vertical stress and the lateral stress in rock interlayer is built as shown in Fig. 7a. It shows that the stress reconstruction follows notably different rules. Vertical stress becomes <8 MPa in the stress release zone. However, mining activity does not achieve the same effect for the lateral stress. Certain extent of lateral stress unexpectedly increases and is apparently higher than the vertical stress (more than 18 MPa). Thus, the mining-induced localized stress concentration in rock interlayer results from the reconstructed lateral stress.

In addition, vector distribution of the major stress in rock interlayer (see Fig. 7b) indicates that major stress in the stress release zone can be separated into two types, the

upward and the downward, based on its direction. Most of the major stress is towards the TZU04 goaf, which makes the upper and middle interlayer rock mass deform upward. A minority of major stress in the lower region makes the interlayer rock mass tend to move downward, which is detrimental to the protected seam exploitation. In production, rock roof over the working face is supported using the hydraulic supports. With the action of downward major stress, rock interlayer becomes easily to cave spontaneously in a large region after the lower seam is extracted. The high stress value provides great power to tightly compress the supports. Meanwhile, the concentrated stress increases the elastic strain energy of unbroken rock mass (Weinberger et al. 2010). A large amount of energy instantly releases along with the roof carving process, which undoubtedly will lead to the supports crushing
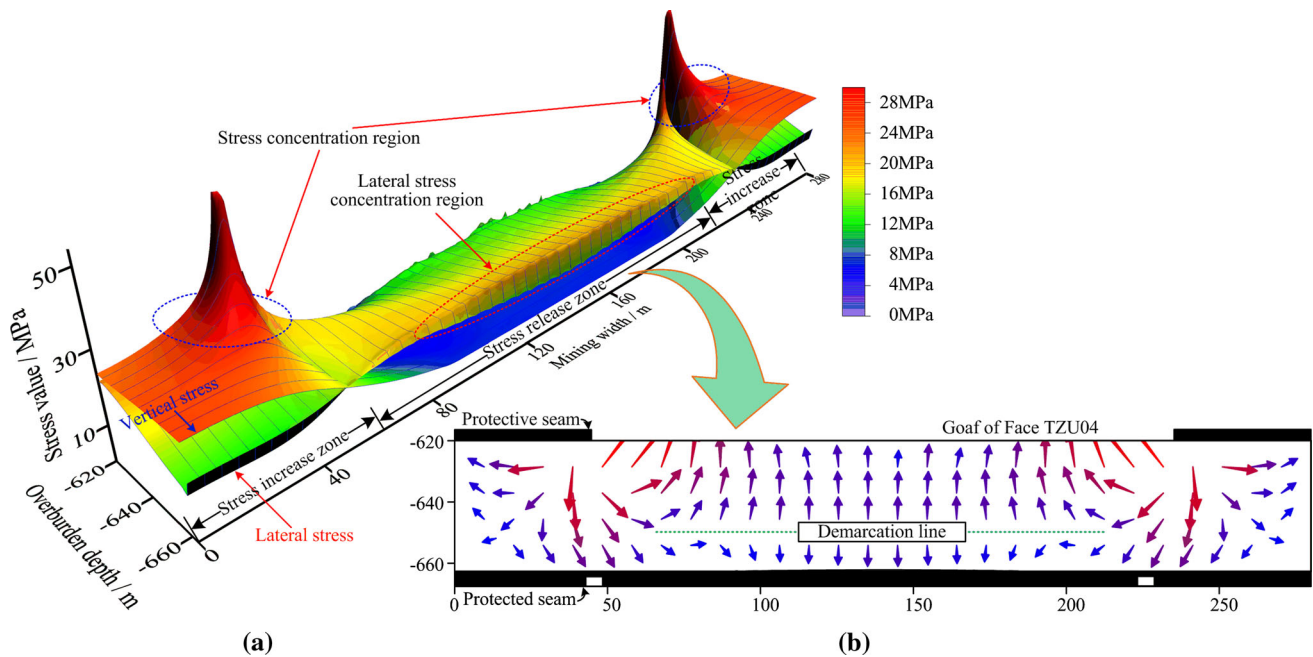
Fig. 7 Comparative redistribution of reconstructed vertical stress, lateral stress and major stress in rock interlayer

accident in protected seam. In particular, as the Fig. 7b indicates, the hydraulic supports under the middle rock interlayer are most likely to be destroyed.

Plastic failure behavior of interlayer rock mass

The reconstructed stress results in the regional plastic deformation and failure behavior of interlayer rock mass, which is shown in Fig. 8. Interlayer rock failure mainly occurs in two regions. One is located in the upper rock stratum. The failure is more serious at distances closer to the TZU04 goaf. Another is located in the lower rock stratum, where the failure extent is greatly lower than the former. As rock interlayer is composed of multiple separated strata and joint surfaces, the renewed failure state changes accordingly to its specific rules. The interaction of structure and stress indicates that the plastic failure behavior breaks the integrity of interlayer rock mass. The range and extent of interlayer rock failure are related to the direction and magnitude of reconstructed major stress. The downward fracture developing angle β is 16°. Upper rock mass fractured seriously under the impact of upward major stress. The rock failure depth d is almost one-third of the aggregate thickness of rock interlayer, and the failure region is about a quarter of the cross-sectional rock area. Moreover, the lower rock interlayer also fractured mildly under the influence of downward major stress. The height of the affected rock mass h is about 2.7 m, and the corresponding fractured region is approximately 2 % of the cross-sectional rock area. Figure 8 also indicates that a higher extent of rock failure behavior generally occurs in

the interlayer where the value of the intrinsic major stress is lower than 15 MPa under these geological and mining conditions.

Mechanical discussion of the localized stress concentration in rock interlayer

A theoretical analysis model

The numerical results reveal the fact of localized stress concentration in rock interlayer and its relevant state and properties. It is necessary to further explore the cause of this stress behavior using mechanical analysis. Similar to the numerical idea, the mechanical model is also considered an integral structure that is constituted by finite rock elements. The difference is that the number of rock elements in the vertical and the lateral directions is countless, i.e., $N_v \rightarrow +\infty$ and $N_l \rightarrow +\infty$. In this case, the volume of each rock element in the model is infinitesimal. Thus, the infinitesimal strain method is introduced into this discussion. Based on the relevant theory (Frederic et al. 2010; Schiffmar 1980; Huang and Sun 2007), the displacement of rock element is assumed to be much smaller than any dimension; its geometry property is assumed unchanged by the deformation. Specifically, the rock element is so infinitesimal that it is simplified to be an isotropically uniform material. This assumption makes the problems easily resolvable based on the established rules. It has been commonly applied in the deformation analysis of the elastic and plastic materials. The mechanical model of rock
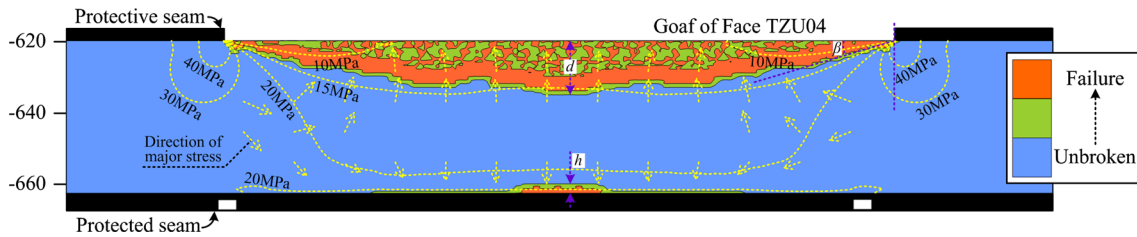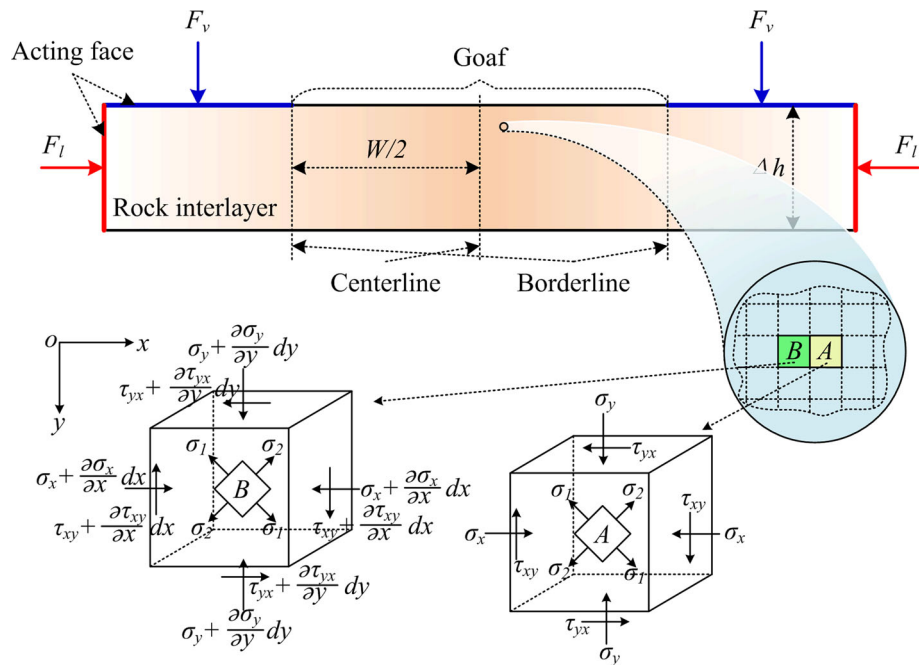
Fig. 8 Failure state of interlayer rock mass

Fig. 9 Mechanical model of rock interlayer extracted from the multi-seam mining structure

interlayer is built as shown in Fig. 9, and a brief description of the infinitesimal strain is provided.

Infinitesimal strain

If the deformation of a continuum body U is nearly equal to its deformation gradient Δu, the body deformation is defined as the infinitesimal deformation in the infinitesimal strain theory (Berndt 2007). Both the body deformation and its deformation gradient are notably smaller than the unity ($\|U\| \approx \|\Delta u\| \ll 1$). By allowing the geometric linearization of Lagrangian finite strain increment E, the nonlinear term of finite strain increment I is neglected (Papadopoulos and Taylor 1994; Jeong and Ramezani 2010). Thus,

$$E = \frac{1}{2}\left(\Delta_X u + (\Delta_X u)^T + \Delta_X u (\Delta_X u)^T\right)$$
$$\approx \frac{1}{2}\left(\Delta_X u + (\Delta_X u)^T\right) \tag{1}$$

The equation implies that there is little difference in the material and spatial coordinates of a given material point in the continuum. The deformation components in material and in space are approximately equal. Thus,

$$\varepsilon = \frac{1}{2}\left((\Delta u + I)^T + \Delta u + I\right) - I \tag{2}$$

where ε is the infinitesimal strain increment. From the expression, the following relation is defined:

$$E_m = \frac{1}{2m}\left[\left((\Delta u + I)^T (\Delta u + I)\right)^m - I\right]$$
$$\approx \frac{1}{2m}\left[\{\Delta u + \Delta u^T + I\}^m - I\right] \approx \frac{1}{2}\left((\Delta u)^T + \Delta u\right) \approx \varepsilon \tag{3}$$

Infinitesimal stress deviation

Stress reconstruction is transient after mining, but strain change is relatively slow. This case provides the mechanical conditions for the deformation of rock elements. The extent is determined by the magnitude of applied force (Boulanger and Hayes 2008). Each individual rock element is not substantive but constrained by its adjacent elements.

Fig. 10 Evolutionary process of interlayer rock failure in the lateral model
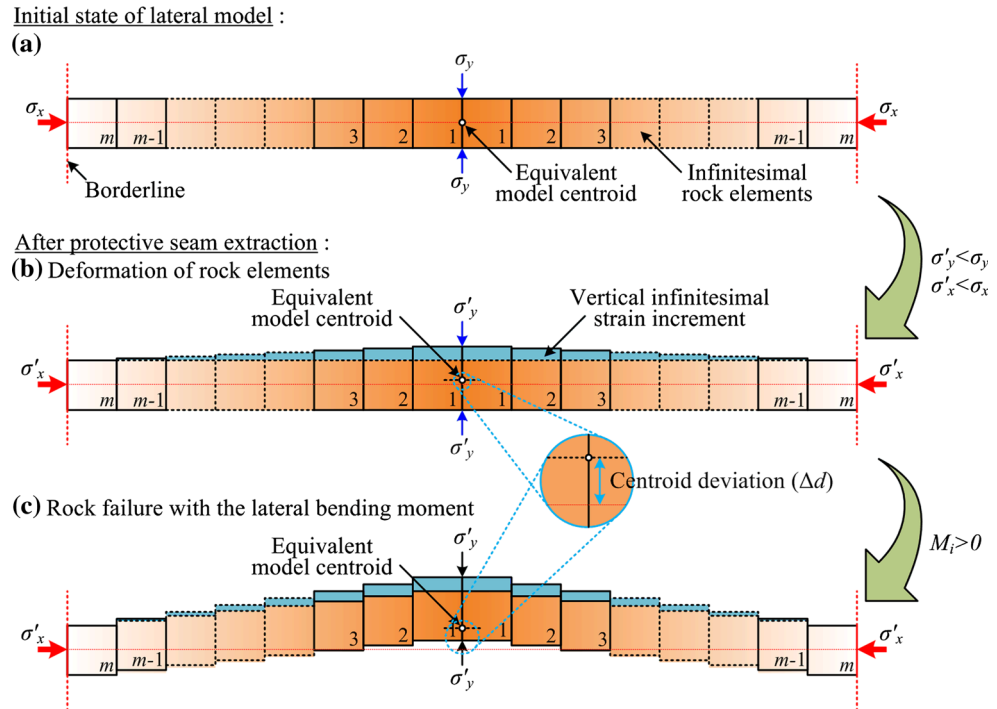
With the action of uneven forces, a small stress deviation generates between two adjacent rock elements (see Fig. 9). The normal stress and shear stress change infinitesimally with the element location in Cartesian coordinates. For the current state, uneven forces have been applied on all infinitesimal rock elements ($\sigma_x > 0$, $\sigma_y > 0$), whereas their infinitesimal strain changes have not started ($\varepsilon_x = \varepsilon_y = 0$).

Infinitesimal deformation and failure of interlayer rock elements

Changes of vertical infinitesimal strain increment

Infinitesimal rock elements in the vertical direction are marked as E_1, E_2, …, E_n. The topmost element E_1 is near the undersurface of TZU04 goaf, and the bottom element E_n is located at a specific depth. The rock elements deformed with the action of unevenly redistributed stress. It is known that the vertical stress decreased in the stress release zone but remained increasing with the overburden depth. Thus, the vertical infinitesimal strain increment decreases with the increased vertical stress. The renewed vertical stress and strain conditions are defined as:

$$\begin{cases} \sigma'_{yn} > \sigma'_{y(n-1)} > \cdots > \sigma'_{y2} > \sigma'_{y1} = 0 \\ \sigma'_{yn} < \sigma_{yn}, \sigma'_{y(n-1)} < \sigma_{y(n-1)}, \ldots, \sigma'_{y2} < \sigma_{y2}, \sigma'_{y1} < \sigma_{y1} \\ \Delta\varepsilon'_{y1} > \Delta\varepsilon'_{y2} > \cdots > \Delta\varepsilon'_{y(n-1)} > \Delta\varepsilon'_{yn} = 0 \end{cases} \quad (4)$$

where σ'_{yi} ($1 \leq i \leq n$, $n \leq N_v$) is the reconstructed vertical stress, $\Delta\varepsilon'_{yi}$ is the vertical infinitesimal strain increment of

rock element, and n is the total number of deformed elements. Infinitesimal strain increments of rock elements are so small that it is supposed that there is a multiple relationship between them, which is represented by k_j ($1 \leq j \leq m$, $m \leq N_1$). Thus, after the rock elements approach a stable strain state, the total strain increment of vertical model $\Delta\varepsilon'_y$ is accumulated as:

$$\Delta\varepsilon'_y = \Delta\varepsilon'_{y1}\left[1 - (1 - k_j)^{n-1}\right]\Big/k_j \quad (5)$$

For the countless vertical models in the lateral direction, their total strain increments $\Delta\varepsilon'_{xjy}$ are then defined as:

$$\Delta\varepsilon'_{xjy} = \Delta\varepsilon'_{xjy1}\left[1 - (1 - k_j)^{n_j-1}\right]\Big/k_j \quad (6)$$

Thus, the following relationship is found:

$$\Delta\varepsilon'_{x1y} > \Delta\varepsilon'_{x2y} > \cdots > \Delta\varepsilon'_{x(m-1)y} > \Delta\varepsilon'_{xmy} = 0 \quad (7)$$

This relationship indicates that the total strain increment of vertical model decreases from the goaf centerline to its borderline (see Fig. 10b). The depth of plastic deformation in rock interlayer increases to its extreme at the goaf centerline.

Action of the lateral bending moment

Infinitesimal rock elements in the lateral direction are marked as E_1, E_2,…, E_m. E_1 is located at the goaf center-line, and E_m is at the goaf borderline. Because the lateral model is constrained on both ends and no free space exits, a

rock element can only squeeze its adjacent elements reciprocally under the action of reconstructed lateral stress σ'_x, which leads to a great deformation in the weak element but a small deformation in the hard element. Compared to the vertical infinitesimal deformation, element deformation in the lateral model is smaller. However, the lateral deformation of rock elements aggravates the instability of lateral rock elements and the range ability of their centroids (Arikan et al. 2010; Park et al. 2012).

The different vertical strain increment makes the centroids of any two adjacent rock elements no longer maintain the same horizon. Thus, a total centroid deviation exists in the lateral model. It is supposed that the vertical strain increment of rock element also has a multiple relationship with its adjacent element in the lateral model, which is represented by k_i. Thus, the total vertical strain increment of lateral model $\Delta\varepsilon'_x$ and its average centroid deviation Δd_i are calculated using the expressions:

$$\Delta\varepsilon'_x = \Delta\varepsilon'_{x1}\left[1 - (1 - k_i)^{m-1}\right]\Big/ k_i \qquad (8)$$

$$\Delta d_i = \Delta\varepsilon'_x / 2m \qquad (9)$$

With the squeezing action of uneven lateral stress, the centroid deviation results in an unbalanced bending moment for the lateral rock elements, which is expressed as:

$$M_i = \int\limits_0^{\frac{1}{2}+\Delta d_i} \sigma'_x \mathrm{d}y - \int\limits_0^{\frac{1}{2}-\Delta d_i} \sigma'_x \mathrm{d}y = 2\sigma'_x \Delta d_i \qquad (10)$$

This relation indicates that the lateral bending moment M_i is greater than zero ($\sigma'_x > 0$, $\Delta d_i > 0$). Rock elements inevitably tend to be extruded and fail under the action of lateral bending moment (see Fig. 10c), which manifests as the interlayer rock failure on the macro level. The extent is related to the magnitude of lateral bending moment and the size of interspace (Tokashiki and Aydan 2011).

Interaction of lateral stress reconstruction and interlayer rock failure

The failure extent of interlayer rock mass also depends on the rock strength (Tenzer et al. 2010). For two adjacent elements loaded by the same force, the element with the lower strength deforms easier than the harder one (Sharifzadeh et al. 2010). On the interface between the rock interlayer and the protected seam, the rock element is harder and more unbreakable than the coal element (Brady and Brown 2004). This difference makes that the infinitesimal deformation of weaker coal elements becomes easier, earlier and more serious than that of the harder rock elements. The deformation of coal elements provides the

weak planes and interspaces for the adjacent rock elements. Thus, the lateral bending moment should increase to force the interlayer rock elements to intrude into the adjacent protected coal seam. Rock failure behavior in the lower part of rock interlayer does not imply that the lateral stress transfers to other regions. On the contrary, rock failure occurs because of the high lateral stress. During the interaction of the stress changes and the rock failure, the lateral stress increases and finally results in the localized stress concentration in this region (see Fig. 11).

It indicates that the decreased vertical stress provides the essential stress conditions for the infinitesimal deformation of rock elements, and the goaf of protective seam offers it sufficient free space and makes the vertical deformation become a main strain state. The vertical infinitesimal strain increment makes the centroids of rock elements no longer maintain the same horizon. Acted on by the increased lateral stress, deformed rock elements result in the final interlayer rock failure. Different failure states occur in different rock strata (Xu and Li 2010). Worse and deeper failure states occur closer to the goaf centerline. It is further found that lateral bending moment is the primary inducing factor of interlayer rock failure, and the vertical infinitesimal strain increments of rock elements are its precondition.

Field investigation

Experiment site and scheme

To verify the numerical and mechanical results, we performed a field experiment in rock interlayer during the coal extraction process of Face TZU04. In the TZ working field, Face TZL03 was designed below Face TZU04. A few connection roadways were tunneled for the ventilation requirements during the excavation of mining roadways. A connection roadway, which was approximately 220 m ahead of TZU04 working face in the horizontal distance, was designated as the experiment site. At its middle location, the stress-monitoring borehole I' and the fracture-observing borehole I, which were 42 mm in diameter and 43 m in height, were drilled upward near two coal walls. The other three fracture-observing boreholes, II, III and IV, were drilled with 20-m interval spacing towards the mining roadway. Fracture development in the inner wall of Holes I, II, III and IV was recorded using the borehole imaging instrument. The observation work was repeated everyday. A customized multipoint unidirectional stress meter manufactured upon the monitoring scenario was applied into Hole I' to detect the changes of lateral stress during the mining process of Face TZU04. It was composed of five stress detectors with the uniform 7-m separation distance.

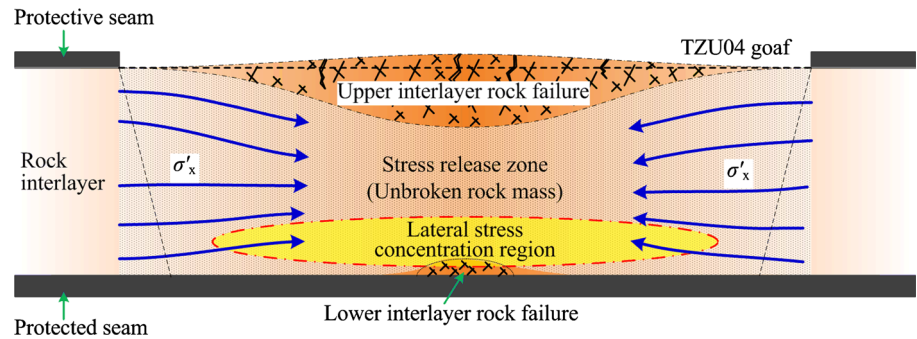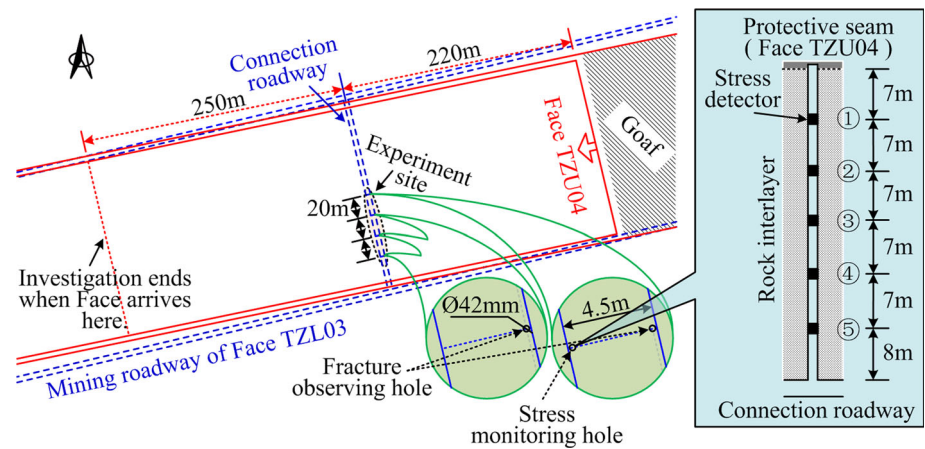**Fig. 11** Action mechanism of stress concentration in the lower interlayer rock mass

Fig. 12 Field experiment site and scheme

In each detector, the highly sensitive hydraulic cylinder was installed. Oil pressure was transduced to stress by the pressure sensor, and then was transmitted to the digital recording equipment. Corresponding stress measuring procedure was mainly consisted of three aspects: the meter installation, the stress monitoring and the data acquisition. Stress detectors were firstly fixed into the right direction and location of borehole I′ with the assistance of guide bar. Immediately following it, an equivalent 15-MPa lateral stress was assigned to each detector accordingly. The advantage of doing this is to hold detectors tightly and to prompt surrounding rock stress to intactly transmit to these detectors as far as possible. Seven to ten days were necessary for the lateral stress on detectors evolving from the initial given level to the natural level. After monitoring data hardly fluctuated, the stress measurement entered into its normal operation stage. The monitoring work was unattended. Required stress data were acquired regularly until the field experiment was ended when the site was 250 m behind the working face. Detailed experiment scheme was shown in Fig. 12.

Results of lateral stress reconstruction and interlayer rock failure

The monitoring results of lateral stress changes in Hole I′ and the interlayer rock failure in Holes I, II, III and IV are shown in Figs. 13 and 14, which show that the lateral stress reconstruction and the rock failure behavior in the stress release zone of rock interlayer were seriously influenced by the protective seam extraction. Figure 13 shows that the lateral stress increased gradually when the stress detectors were ahead of working face. It decreased by a small amount in the lower rock stratum. After the TZU04 working face passed over the connection roadway, the lateral stress redistribution dramatically reversed in a short period. Lateral stress in the upper rock stratum sharply decreased, but the lateral stress in the lower rock stratum obviously increased. The lower rock stratum corresponded to the higher lateral stress, which indicates the forming process of localized stress concentration in rock interlayer. Figure 14 shows that the inner wall of observing holes suffered distinct destruction during the mining disturbance. The destruction level is separated into the badly destroyed level (Fig. 14a), the moderately destroyed level (Fig. 14b) and the slightly destroyed level (Fig. 14c). Fractures fully developed in the upper part of observing holes. The hole had more fractures closer to its top. Hole I at the goaf centerline was destroyed more seriously than the others, and the fracture development in Hole IV was relatively the slightest. In addition, the extent of fracture development in the lower part of holes (Fig. 14e) was not identified because of the secondary effect induced by the excavation activity of connection roadway. It is found that as the

Fig. 13 Lateral stress changes and fracture developing state in rock interlayer during the TZU04 mining process
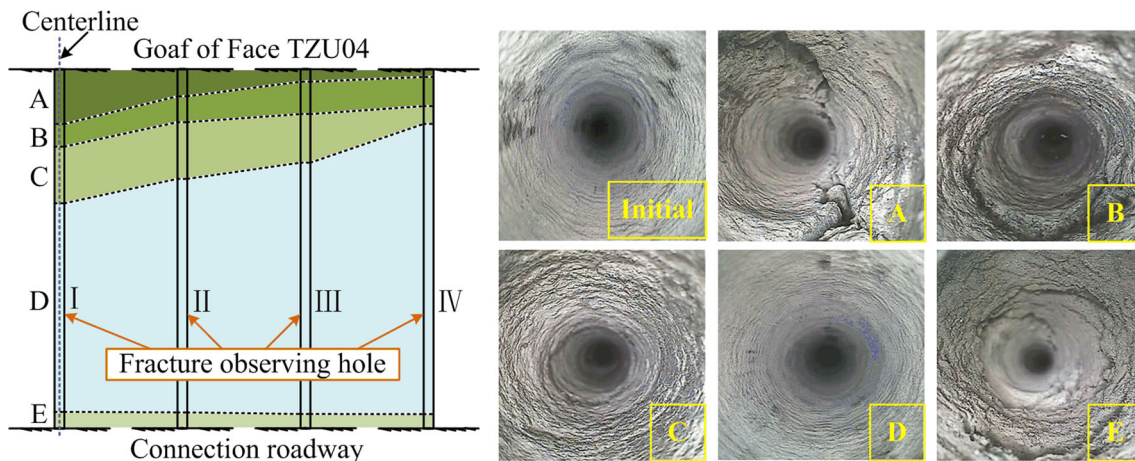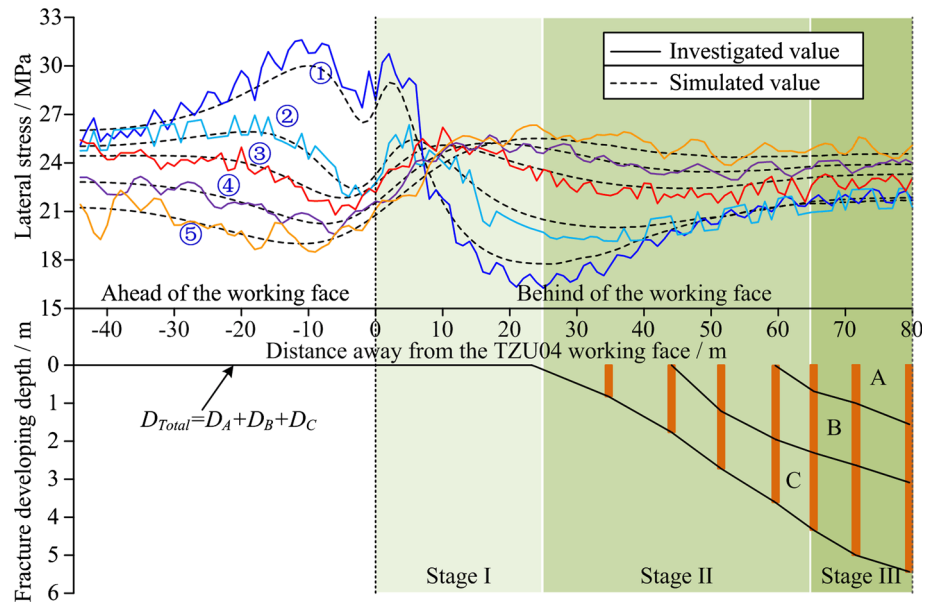

Fig. 14 Final failure state of interlayer rock mass in the boreholes I, II, III and IV

distance from the TZU04 working face increased, the lateral stress no longer changed too much and gradually remained at a stable high level. The total fracture developing depth D_{Total} also increased to a specific value.

Field investigation indicates that the lateral stress in rock interlayer increases to a high level after the protective seam exploitation. It results in the localized stress concentration in the lower rock stratum. Localized stress concentration in the stress release zone of rock interlayer is induced from the interaction of lateral stress reconstruction and the interlayer rock failure. Lateral stress changes with the influence of protective seam exploitation (stage I in Fig. 13). Then, rock failure behavior occurs with the action of unevenly distributed stress state (stage II in Fig. 13), which forces the lateral stress to further reconstruct gradually (stage III in Fig. 13). This interaction continues until an equilibrium state of stress and strain is achieved in rock

interlayer. Lateral stress reconstruction provides the mechanical requirements for interlayer rock failure; this plastic failure behavior further promotes the stress concentration in the stress release zone. It indicates that the numerical and mechanical results are consistent with the field investigation results.

Prevention measures for the localized stress concentration in rock interlayer

The discussion and investigation confirm that the localized stress concentration in rock interlayer results in the supports crushing accident during the protected seam exploitation. Thus, we propose five control measures to prevent the recurrence of this stress behavior and mining accidents during the coal extraction activity of TZL03 working face.
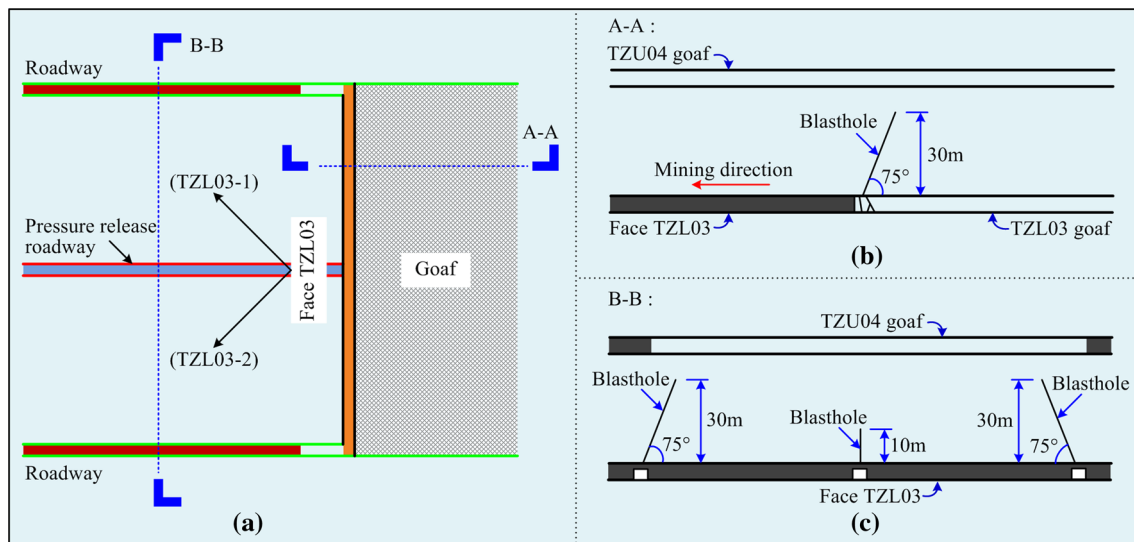
Fig. 15 Control measures applied in Face TZL03 to prevent the localized stress concentration

Determine the top-coal caving as the mining method

The 5-m thickness of TZL coal seam indicates that the full-seam exploitation and the top-coal caving are both applicable mining methods. Using the former, the bottom of rock interlayer will have a surface-to-surface contact with the top surface of hydraulic supports. In this case, the supports are easily crushed tightly once the interlayer rock mass caves. However, this situation can be relieved using the top-coal caving. Top-coal caving disturbs the reconstructed stress state in rock interlayer, provides a huge free space for the deformation and failure of interlayer rock mass, provides a buffering effect for the energy release induced by the stress concentration, and disables the released energy from acting directly upon the hydraulic supports. This method is more suitable for exploiting the TZL coal seam.

Select the appropriate hydraulic supports

Based on the mining method, the changes of seam thickness and dip angle, and the hydraulic supporting force and mode, ZFS6200/18/35(C) coal caving hydraulic support is optimally selected for the exploitation in Face TZL03. Its working resistance is 6,000–6,250 kN, which satisfies the supporting requirements. Its support height is 1,800–3,500 mm. Thus, a 3-m mining height is applicable, and the residual coal body above supports is treated as the top coal. It is necessary to reasonably adjust the height of hydraulic supports to suit the roof weight and the geological structures.

Optimize the layout of mining roadways

Because the stress concentrates in the lower part of rock interlayer, a pressure-release roadway is suggested to be supplementarily excavated in the middle face to disturb the reconstructed stress state (see Fig. 15a). In severe cases, Face TZL03 can be divided into two small working faces and extracted separately with a small stagger interval. This method reduces the overall impact of localized stress concentration on the exploitation in Face TZL03.

Intervene artificially the periodic roof pressure

Protected seam exploitation in other working fields indicates that the average distance of periodic roof pressure is 35–50 m. To avoid the stress superposition of localized stress concentration and the newborn periodic roof pressure, a roof-blasting operation above the TZL03 working face is implemented. Drilling parameters of blastholes are shown in the Fig. 15b. This operation breaks the hanging roof in advance, which plays an important role to shorten the period and reduce the intensity of roof pressure.

Implement the roof-blasting operation in the roadways

High lateral stress in the two stress increase zones generates a squeezing action on the interlayer rock mass in stress release zone. To weaken this stress effect, a roof-blasting operation is implemented in three roadways to break the integrality of rock interlayer (see Fig. 15c). In front of the TZL03 working face, blasting scheme is repeated every

15 m in mining direction. After the artificial intervention, plastic failure extent of the interlayer rock mass will increase, whereas the stress concentration degree in the lower part of rock interlayer will decrease.

Conclusions

In the deep multi-seam mining structure, protected coal seam in the stress release zone cannot always be safely extracted. Based on the above discussion and investigation, the following points can be concluded:

1. After the exploitation in protective seam, the vertical stress decreases significantly in the stress release zone of rock interlayer. However, the lateral stress increases with the overburden depth and concentrates on its lower part. A lower rock stratum corresponds to a greater stress concentration degree. This stress behavior increases the elastic strain energy of unbroken interlayer rock mass. Hydraulic supports under the middle rock interlayer are most likely to be destroyed.

2. The failure behavior of rock interlayer occurs in its upper and lower parts. It breaks the integrity of interlayer rock mass. The more serious rock failures occur closer to the goaf centerline of protective seam. Different plastic failure behaviors occur in different rock strata. The failure range and extent depend on the rock strength, the direction and magnitude of reconstructed major stress. Lateral bending moment is the primary inducing factor of interlayer rock failure behavior; the vertical strain increment of infinitesimal rock element is its precondition.

3. The mining-induced localized stress concentration in the stress release zone of rock interlayer results from the interaction of lateral stress reconstruction and interlayer rock failure. This interaction continues until an equilibrium state of stress and strain is achieved. The lateral stress reconstruction provides the mechanical requirements for the interlayer rock failure; the plastic failure behavior further promotes the localized stress concentration in stress release zone.

4. It must be noted that prevention measures for the localized stress concentration in rock interlayer are being applied in the coal extraction process of Face TZL03. Relevant control effects will be timely checked and continuously studied in future researches. The findings of this study were obtained based on the specific geologic and mining conditions in Jining deep mine; similar studies will be performed in other coal mines to promote a more systematic exploration of this stress concentration behavior in the deep multi-seam mining structure.

References

Arikan F, Yoleri F, Sezer S, Caglan D, Biliyul B (2010) Geotechnical assessments of the stability of slopes at the Cakmakkaya and Damar open pit mines (Turkey): a case study. Environ Earth Sci 61:741–755

Berndt R (2007) Representations of linear groups: an introduction based on examples from physics and number theory. Vieweg, Germany

Boulanger P, Hayes M (2008) Determination of the infinitesimal strain tensor from shears and elongations. J Elast 92:209–216

Brady BH, Brown ET (2004) Rock mechanics for underground mining. Kluwer Academic, Germany

China Ministry of Coal Industry (1987) National provisional rules of safe mining in rock burst seam. China Ministry of Coal Industry, Beijing

Dou LM, Zhao CG, Yang SG, Wu XR (2006) Prevention and control of rock burst in coal mine. China University of Mining and Technology Press, Xuzhou

Frederic PM, Agnes FV, John MB (2010) Infinitesimal strain theory. Alphascript Publishing, Germany

Guo H, Yuan L, Shen BT, Qu QD, Xue JH (2012) Mining-induced strata stress changes, fractures and gas flow dynamics in multi-seam longwall mining. Int J Rock Mech Min Sci 54:129–139

Gurbuz A (2011) A new approximation in determination of vertical displacement behavior of a concrete-faced rockfill dam. Environ Earth Sci 64:883–892

Hashash YMA, Cording EJ, Oh J (2002) Analysis of shearing of a rock ridge. Int J Rock Mech Min Sci 39:945–957

Huang ZP, Sun L (2007) Size-dependent effective properties of a heterogeneous material with interface energy effect: from finite deformation theory to infinitesimal strain analysis. Acta Mech 190:151–163

Itasca Consulting Group, Inc, 2005. FLAC User's Guide

Jeong J, Ramezani H (2010) Enhanced numerical study of infinitesimal non-linear Cosserat theory based on the grain size length scale assumption. Comput Methods Appl Mech Eng 199:45–48

Jia TR, Zhang ZM, Tang CA, Zhang YJ (2013) Numerical simulation of stress-relief effects of protective layer extraction. Arch Min Sci 58:521–540

Khare S, Rao YV, Murthy CS, Vardhan H (2006) Multiple seam mining: a critical review. J Mines Met Fuels 54:327–329

Lempp C, Shams KM, Jahr N (2012) Approaches to stress monitoring in deep boreholes for future CCS projects. Environ Earth Sci 67:435–445

Liu YK, Zhou FB, Liu L, Liu C, Hu SY (2011) An experimental and numerical investigation on the deformation of overlying coal seams above double-seam extraction for controlling coal mine methane emissions. Int J Coal Geol 87:139–149

Lobanova TV (2008) Geomechanical state of the rock mass at the Tashtagol mine in the course of nucleation and manifestation of rock bursts. J Min Sci 44:146–154

Lourenco SDN, Wang GH, Chu JA (2011) Aspects of sand behaviour by modified constant shear drained tests. Environ Earth Sci 62:865–870

Nasedkina AA, Nasedkin AV, Iovane G (2008) A model for hydrodynamic influence on a multi-layer deformable coal seam. Comput Mech 41:379–389

Nasedkina AA, Nasedkin AV, Iovane G (2009) Modeling and finite element analysis of the nonstationary action on a multi-layer poroelastic seam with nonlinear geomechanical properties. J Min Sci 45:324–333

Papadopoulos P, Taylor RL (1994) On the application of multistep integration methods to infinitesimal elastoplasticity. Int J Numer Methods Eng 37:3169–3184

Park HJ, Um JG, Woo I, Kim JW (2012) The evaluation of the probability of rock wedge failure using the point estimate method. Environ Earth Sci 65:353–361

Qin SQ, Jiao JJ, Tang CA, Li ZG (2006) Instability leading to coal bumps and nonlinear evolutionary mechanisms for a coal-pillar-and-roof system. Int J Solids Struct 43:7407–7423

Schiffmar RL (1980) Finite and infinitesimal strain consolidation. J Geotech Geoenviron Eng 106:203–207

Sharifzadeh M, Sharifi M, Delbari SM (2010) Back analysis of an excavated slope failure in highly fractured rock mass: the case study of Kargar slope failure (Iran). Environ Earth Sci 60:183–192

Sun HY, Zhao Y, Shang YQ, Zhong J (2013) Field measurement and failure forecast during the remediation of a failed cut slope. Environ Earth Sci 69:2179–2187

Tati BB (2011) Multi-seam coal mining. J S Afr Inst Min Metall 111:231–242

Tenzer H, Park CH, Kolditz O, McDermott CI (2010) Application of the geomechanical facies approach and comparison of exploration and evaluation methods used at Soultz-sous-Forts (France) and Spa Urach (Germany) geothermal sites. Environ Earth Sci 61:853–880

Tokashiki N, Aydan O (2011) Kita-Uebaru natural rock slope failure and its back analysis. Environ Earth Sci 62:25–31

Wang JC, Zhao HB (2010) Numerical simulation on deformation rule of protected coal seam under upper protective seam method. Disaster Adv 3:383–387

Weinberger R, Eyal Y, Mortimer N (2010) Formation of systematic joints in metamorphic rocks due to release of residual elastic strain energy, Otago Schist, New Zealand. J Struct Geol 32:288–305

Wu JH, Pan YW (2013) Three-dimensional in situ stress evaluation using a new under-coring technique: the Tseng-Wen Reservoir Transbasin water tunnel. Environ Earth Sci 68:77–86

Xiong ZQ, Li HM, Yuan C (2008) Study on technology of far-distance protective coal seam mining and pressure-relief gas extraction. Prog Saf Sci Technol Ser 7:1470–1473

Xu JC, Li N (2010) Influence of continuous rainfall on surrounding rock-initial support system of shallow decomposed-rock tunnel. Environ Earth Sci 61:1751–1759

Yang TH, Xu T, Liu HY, Tang CA, Shi BM, Yu QX (2011a) Stress-damage-flow coupling model and its application to pressure relief coal bed methane in deep coal seam. Int J Coal Geol 86:357–366

Yang W, Lin BQ, Qu YA, Li ZW, Zhai C, Jia LL, Zhao WQ (2011b) Stress evolution with time and space during mining of a coal seam. Int J Rock Mech Min Sci 48:1145–1152

Yang W, Lin BQ, Qu YA, Zhao S, Zhai C, Jia LL, Zhao WQ (2011c) Mechanism of strata deformation under protective seam and its application for relieved methane control. Int J Coal Geol 85:300–306

Yin ZQ, Li XB, Jin JF, He XQ, Du K (2012) Failure characteristics of high stress rock induced by impact disturbance under confining pressure unloading. Trans Nonferrous Met Soc China 22:175–184

Yuan ZG, Wang HT, Fan XG, Liu NP, Liu JC (2010) Numerical simulation for protection range of steep inclined upper-protective layer of pitching oblique mining. Prog Saf Sci Technol Ser 8:2535–2541

Zhang LY, Deng KZ, Zhu CG, Xing ZQ (2011) Analysis of stability of coal pillars with multi-coal seam strip mining. Trans Nonferrous Met Soc China 21:549–555